To appear in *Molecular Physics*
Vol. 00, No. 00, Month 2015, 1–16

Long-range correction for dipolar fluids at planar interfaces

Stephan Werth, Martin Horsch* and Hans Hasse

Laboratory of Engineering Thermodynamics, Department of Mechanical and Process Engineering, University of Kaiserslautern, Erwin-Schrödinger-Str. 44, 67663 Kaiserslautern, Germany

(*submitted May 2015*)

A slab-based long-range correction for dipolar interactions in molecular dynamics simulation of systems with a planar geometry is presented and applied to simulate vapor-liquid interfaces. The present approach is validated with respect to the saturated liquid density and the surface tension of the Stockmayer fluid and a molecular model for ethylene oxide. The simulation results exhibit no dependence on the cutoff radius for radii down to 1 nm, proving that the long-range correction accurately captures the influence of the dipole moment on the intermolecular interaction energies and forces as well as the virial and the surface tension.

Keywords: long-range correction; surface tension; planar interfaces; dipole; Stockmayer fluid

1. Introduction

The surface tension is an important mechanical and thermodynamic property of fluids. Despite its importance, there are only few reliable studies on the surface tension by molecular simulation, compared to the work done on bulk properties of the vapor-liquid equilibrium. The calculation of interfacial properties, such as the surface tension, is usually done in the canonical ensemble, with a liquid film in the center of the simulation volume, surrounded by vapor phases [1–7].

In molecular simulations of a homogeneous bulk fluid, the long-range part of the force field acting on a single molecule averages out beyond a certain cut-off r_c, and straightforward mean-field approximations can be applied to compute the long-range contribution to the energy and the pressure [8]. For electroneutral molecules, including dipoles, these corrections can e.g. be treated with the reaction field method [9]. Molecular simulations with interfaces are more challenging due to the inhomogeneity of the simulation volume which causes e.g. the approximation behind the reaction field method to break down [10].

For dispersive interactions, like the Lennard-Jones potential, various long-range correction (LRC) approaches exist which are known to be accurate for planar fluid interfaces, ranging from Ewald summation techniques [11, 12], the Fast Multipole Method (FMM) [13] and Multilevel Summation (MLS) [14] to slab-based LRC techniques [15–17]. Ewald summation techniques have the disadvantage that even highly optimized codes scale with $\mathcal{O}(N^{3/2})$ in terms of the number of molecules N [18, 19] and more sophisticated methods like PPPM Ewald scale with $\mathcal{O}(N \log N)$ [12, 20]. Methods like FMM, MLS and slab-based LRCs have a more favorable linear

*Corresponding author. Email: martin.horsch@mv.uni-kl.de

ISSN: 0892-7022 print/ISSN 1029-0435 online

DOI: 10.1080/0892702YYxxxxxxxx
http://www.informaworld.com

scaling, i.e. $\mathcal{O}(N)$ [13, 14, 17, 21]. Additionally to the scaling behavior with the number of molecules, the scaling with the number of processing units of the Ewald summation techniques is unfavorable due to the large amount of communication needed for the Fourier transform [22]. In terms of the thermodynamic results, the different methods deliver a similar degree of accuracy for Lennard-Jones systems [12, 14, 16, 17].

There a more than 50 accurate molecular models for real fluids from previous work of our group based on multi-center Lennard-Jones plus point dipole force fields, which were adjusted to bulk properties of the vapor-liquid equilibrium [23–29]. For a comprehensive review of this modelling approach, the reader is pointed to work of Merker et al. [30]. Dipole-dipole interactions decay with r^{-6} for long distances, like the Lennard-Jones potential [31, 32]. Molecular simulations of heterogeneous systems (e.g. at interfaces) for dipolar fluid models are usually conducted with an Ewald summation for the treatment of the long-range interactions [33–36]. At planar interfaces, however, a more efficient LRC can be used that evaluates the density profile, exploiting the planar geometry of the system. Such a method is developed in the present work.

For this purpose, we combine the slab-based LRC approach by Janeček [16] with an angle averaged dipole-dipole interaction [31, 32]. This novel and efficient LRC is applied here to the Stockmayer fluid [37] and a molecular model of ethylene oxide [25].

2. Simulation Method

The intermolecular pair potentials studied in the present work consist of Lennard-Jones sites and a point dipole. The Stockmayer fluids consists of a single Lennard-Jones site and superimposed point dipole [37]. The molecular model of ethylene oxide by Eckl et al. is modeled by three Lennard-Jones sites, i.e. two for the two methylene groups and one for the oxygen atom, and a superimposed dipole in the center of mass [25]. The pair potential is given as a sum of the different interaction types

$$u_{ij} = u_{ij}^{\mathrm{LJ}} + u_{ij}^{\mathrm{Dipole}}. \tag{1}$$

The Lennard-Jones potential

$$u_{ij}^{\mathrm{LJ}} = 4\epsilon \left[\left(\frac{\sigma}{r_{ij}} \right)^{12} - \left(\frac{\sigma}{r_{ij}} \right)^{6} \right], \tag{2}$$

has two parameters, the energy parameter ϵ and the size parameter σ. The dipole-dipole interaction is given by

$$u_{ij}^{\mathrm{Dipole}} = \frac{\mu_i \mu_j}{r_{ij}^3} \left(\cos\gamma_{ij} - 3\cos\vartheta_i \cos\vartheta_j \right), \tag{3}$$

with the dipole moments μ_i and μ_j, the relative orientations ϑ_i and ϑ_i between the distance vector r_{ij} and the dipole orientations, the azimuthal angle of the two dipole orientations γ_{ij} [38] and $1/4\pi\epsilon_0 = 1$.

The intermolecular potential is usually truncated in molecular simulations, for numerical reasons. The error made by this approximation has to be corrected with a LRC. For the Lennard-Jones interactions a slab-based LRC from previous work of our group is used in the present study [17]. For the dipolar interactions a novel slab-based LRC is presented.

On the long range the dependence of the interaction on the orientation of the molecules averages out, due to the large number of interaction partners, assuming that the fluid molecules do not have a preferred orientation. For the LRC the angle averaged version of equation (3) is therefore applicable, which is given by

$$u_{ij}^{\text{Dipole}} = \frac{1}{3k_{\text{B}}T}\frac{\mu_i^2\mu_j^2}{r_{ij}^6}, \tag{4}$$

with the Boltzmann constant k_{B} and the temperature T [31, 32].

In the present work molecular simulation of planar interfaces are conducted, i.e. the density only changes in the direction normal to the interface, which corresponds to the y-direction here. The LRC is based on the density profile $\rho(y)$. The correction term U_i^{LRC} is a sum over all N_{s} slabs in the simulation volume, including periodic boundary conditions. It is calculated between the molecule i and the molecules in slab k by

$$U_i^{\text{LRC}} = \frac{1}{2}\sum_k^{N_{\text{s}}} 2\pi\rho\left(y_k\right)\Delta y \int_{r'}^{\infty} \mathrm{d}r \frac{\mu_i^2\mu_j^2}{3k_{\text{B}}Tr^6} r, \tag{5}$$

where $\rho\left(y_k\right)$ denotes the density in slab k and Δy is the slab thickness. The factor $1/2$ in equation (5) is due to the fact that the potential energy is defined by a pair potential, one half of which can be assigned to each interacting molecule. The radial distribution function was assumed to be unity beyond the cutoff radius. According to Siperstein et al. [39], the lower integration bound r' has to be selected in a way to prevent a double calculation. If the normal distance $\xi = |y_i - y_k|$ between a molecule i and the slab k is smaller than the cutoff radius, the cutoff radius has to be used as the lower integration bound, otherwise ξ is used, i.e.

$$r' = \begin{cases} \xi, & \text{if} \quad \xi > r_c \\ r_c, & \text{instead.} \end{cases} \tag{6}$$

The procedure is identical to the procedure for the Lennard-Jones potential [16, 17]. The only difference is the potential model.

Performing the integration in equation (5) gives

$$\begin{aligned} U_i^{\text{LRC}} &= -\sum_k^{N_{\text{s}}} \pi\rho\left(y_k\right)\Delta y \int_{r'}^{\infty} \mathrm{d}r \frac{\mu_i^2\mu_j^2}{3k_{\text{B}}Tr^6} r \\ &= -\sum_k^{N_{\text{s}}} \pi\rho\left(y_k\right)\Delta y \frac{\mu_i^2\mu_j^2}{12k_{\text{B}}Tr'^4}. \end{aligned} \tag{7}$$

The correction for the forces is given in a similar manner

$$F_i^{\mathrm{LRC}} = -\sum_k^{N_\mathrm{s}} \pi\rho\left(y_k\right)\Delta y \int_{r'}^{\infty} \mathrm{d}r \frac{\partial u}{\partial r}\frac{\xi}{r} r$$
$$= -\sum_k^{N_\mathrm{s}} \pi\rho\left(y_k\right)\Delta y \frac{\mu_i^2\mu_j^2}{3k_\mathrm{B}Tr'^6}\xi. \tag{8}$$

At a planar interface, the pressure is not isotropic. If the pressure is calculated by a virial approach [40], the components of the tangential and normal direction of the virial tensor are different, and the same holds true for the LRCs of the respective spatial directions. The LRC for the normal virial, which corresponds to the y-direction, is

$$\Pi_{N,i}^{\mathrm{LRC}} = -\frac{1}{2}\sum_k^{N_\mathrm{s}} \pi\rho\left(y_k\right)\Delta y \int_{r'}^{\infty} \mathrm{d}r \frac{\partial u}{\partial r}\frac{\xi^2}{r} r$$
$$= -\sum_k^{N_\mathrm{s}} \pi\rho\left(y_k\right)\Delta y \frac{\mu_i^2\mu_j^2}{6k_\mathrm{B}Tr'^6}\xi^2. \tag{9}$$

The tangential virial, corresponding to the x- and z- direction here, is

$$\Pi_{T,i}^{\mathrm{LRC}} = -\frac{1}{4}\sum_k^{N_\mathrm{s}} \pi\rho\left(y_k\right)\Delta y \int_{r'}^{\infty} \mathrm{d}r \frac{\partial u}{\partial r}\frac{r^2-\xi^2}{r} r$$
$$= -\sum_k^{N_\mathrm{s}} \pi\rho\left(y_k\right)\Delta y \frac{\mu_i^2\mu_j^2}{24k_\mathrm{B}Tr'^6}\left(3r^2-2\xi^2\right). \tag{10}$$

The correction terms differ only in the prefactors compared with the slab-based LRC for the Lennard-Jones interactions, if the r^{-12} terms are neglected.

3. Simulation details

The above correction terms were implemented in the *ls*1 *mardyn* molecular dynamics code [41, 42] to validate the present LRC approach. The equations of motion were solved by a leapfrog integrator [43] with a reduced time step of $\Delta t = 0.001\ \sigma\sqrt{m/\epsilon}$ for the Stockmayer fluid and $\Delta t = 1$ fs for the ethylene oxide model [25] which were studied as test cases. Simulations were conducted in the canonical ensemble with $N = 16{,}000$ molecules. The liquid phase was in the center of the simulation volume, surrounded by vapor on both sides. The elongation of the simulation volume normal to the interface was 80 σ to limit the influence of finite size effects [44]. The spatial extension in the other directions was at least 20 σ. A numerical resolution of the density profile given by a thickness of the LRC slabs of $\Delta y = 0.1\ \sigma$ was used throughout. For ethylene oxide, the $\sigma_{\mathrm{CH_2}}$ value of the methylene groups is used as the reference σ. The equilibration was conducted for 500,000 time steps and the production runs for 2,500,000 time steps to reduce statistical uncertainties. The statistical errors were estimated to be three times the standard deviation of five block averages [45], each over 500,000 time steps. The saturated

densities were calculated as an average over the respective phase excluding the area close to the interface, i.e. the area where the first derivative of the density with respect to the y coordinate is not zero. The surface tension was computed from the deviation between the normal and the tangential diagonal components of the overall pressure tensor [46, 47]. Thereby, the tangential pressure p_T was determined by averaging over the two tangential components of the pressure tensor.

$$\gamma = \Pi_N - \Pi_T = \frac{1}{2A} \int_{-\infty}^{\infty} \mathrm{d}y \, (p_N - p_T) \tag{11}$$

Series of molecular dynamics simulations were carried out for the Stockmayer fluid with different dipolar strengths and ethylene oxide. Three different approaches are compared regarding the influence of the cutoff radius: Simulations without any LRC, simulations with a LRC only for the Lennard-Jones interactions and simulations with a LRC for the Lennard-Jones plus the dipolar interactions.

4. Results

Figure 1 shows the density profile for the Stockmayer fluid with a dipole moment $\mu^2 = 5\ \epsilon\sigma^3$ for a temperature close to the triple point temperature. The simulations have been performed with the present LRC approach. The force correction F^{LRC} due to the LRC for the dipolar interactions is shown for various cutoff radii. F^{LRC} is negligible in the liquid and the vapor phase, which has to be expected, since the molecules have a nearly homogeneous neighborhood. At the interface F^{LRC} exhibits a maximum due to the strong inhomogeneity, with the very dense liquid phase on the one side and the sparse vapor phase on the other side. The range of influence of F^{LRC} is approximately 10 σ, which means that molecular simulations with a cutoff radius $r_c = 10\ \sigma$ should be sufficient without any LRC at low temperatures. Molecular simulations are usually performed with a cutoff radius of half that size [48–52] and the computing time scales with r_c^3. Increasing the temperature increases the interfacial width and the range of the long-range interactions.

[Figure 1 about here.]

Figure 2 shows the saturated liquid density of the Stockmayer fluid with $\mu^2 = 5\ \epsilon\sigma^3$ over the cutoff radius, for three temperatures from near the triple point up to 0.92 T_c, where $T_c = 2.29\ \epsilon/k_{\mathrm{B}}$ is the critical temperature [53]. The dipole moment of $\mu^2 = 5\ \epsilon\sigma^3$ is larger than the value for any real fluid modelled by a Stockmayer fluid [29, 54–56]. The results for the saturated liquid density that were determined with the present novel LRC scheme show hardly any dependence on the cutoff radius even down to $r_c = 2.5\ \sigma$, while the other approaches show significant deviations from the reference bulk saturated liquid density [53].

[Figure 2 about here.]

It is known that Stockmayer fluids with large dipole moments tend to form structured chains [57, 58]. Nonetheless, to check the performance of the LRC, the dipole moment was increased to $\mu^2 = 16\ \epsilon\sigma^3$. The temperature ranged from close to the triple point up to 0.9 T_c, where $T_c = 4.68\ \epsilon/k_{\mathrm{B}}$ [58]. Figure 3 shows the results for the saturated liquid density. A cutoff radius of $r_c = 3.5\ \sigma$ is needed for the Lennard-Jones plus dipolar LRC to yield accurate results. However, the simulation results for both other approaches show much larger deviations over

the entire temperature range, which proves that the present LRC substantially increases the simulation accuracy even under extreme conditions.

[Figure 3 about here.]

As a test case for real fluids, ethylene oxide is considered. The cutoff radius is expressed here in multiples of the σ value of the methylene interaction sites, i.e. σ = 3.5266 Å, to make it better comparable with the simulation series for the Stockmayer fluid. The reduced cutoff radius was varied from 2.5 to 6 σ, corresponding to 0.88 nm to 2.12 nm. Simulations were performed for 200, 300 and 400 K, i.e. from triple point temperature up to 0.85 T_c, where T_c = 469.2 K [60]. Figure 4 shows the results for the saturated liquid density. The results with the LRC for the Lennard-Jones plus dipolar interactions are even better than the results for the Stockmayer fluid with $\mu^2 = 5\ \epsilon\sigma^3$, leading to cutoff independent results down to r_c = 2.5 σ. The simulations with no LRC or a LRC for the Lennard-Jones potential only, show a noticeable deviation from the reference [25].

[Figure 4 about here.]

The basic assumption behind the LRC is a planar interface and no preferred orientation of the molecules. To proof that this is valid, Figure 5 shows the orientation of the molecules over the y coordinate.

[Figure 5 about here.]

The orientational parameter P was introduced by Harris [61]

$$P(y) = 3(\cos^2\theta - 1) \tag{12}$$

,where $P(y) = -0.5$ means that the molecules are oriented parallel to the interface, $P(y) = 1$ normal to the interface, and $P(y) = 0$ means that the molecules are randomly oriented. For all fluids investigated in the present work, the orientation was evaluated at the lowest temperature and a cutoff radius of $r_c = 6\ \sigma$. No preferred orientation is found, which confirms that the present approach is applicable. Due to the low temperature and the corresponding low vapor density, the fluctuations of the order parameter is relatively high in the vapor phase. Preferred orientations occur if an external field is present. In these cases, a LRC which takes the orientation explicitly into account is necessary [36, 59].

Another very important property of the vapor-liquid equilibrium is the surface tension, which is much more sensitive to the truncation than the saturated liquid density. The surface tension of the fluids discussed above was determined with the three different approaches. Figure 6 shows the surface tension over the cutoff radius for the two Stockmayer fluids and ethylene oxide for one selected temperature of each fluid. The surface tension determined with the Lennard-Jones plus dipolar LRC scatters around a single value for the Stockmayer fluid with $\mu^2 = 5\ \epsilon\sigma^3$ and ethylene oxide, showing no real dependence on the cutoff radius at least down to about 3 σ, while both other methods show a significant dependence on the cutoff radius. The surface tension of the Stockmayer fluid with $\mu^2 = 16\ \epsilon\sigma^3$ is overestimated with the Lennard-Jones plus dipolar LRC, as well as the saturated liquid density, below $r_c = 3.5\ \sigma$. The other approaches show a large dependence of the surface tension on the cutoff radius and the surface tension values do not converge, even for a large cutoff radius up to $r_c = 6\ \sigma$.

[Figure 6 about here.]

Like the slab based LRC from previous work for the Lennard-Jones interactions [17], the computing time of the slab-based LRC for dipolar interactions scales almost linearly with number of molecules. The amount of additional computing time is approximately 10 % at the lowest cutoff radius, and the computing time for the LRC is independent of the chosen cutoff radius. On the other hand, the overall computing time is very significantly reduced by reducing the cutoff radius, since much fewer interactions have to be evaluated explicitly. With the present LRC approach, this is reliably possible even for dipolar fluids. In absolute terms, independent of the cutoff radius, only a very small amount of computing time is used for the calculation of the long-range correction.

5. Conclusion

In the present work, a new slab-based LRC approach for dipolar fluids and planar interfaces was presented. It was applied to molecular models consisting of Lennard-Jones sites and a dipole. The influence of the LRC on the saturated liquid density and the surface tension was determined. The present LRC approach yields good results for both properties and shows no dependence on the choice of the cutoff radius down to small radii of about 2.5 σ. The LRC reduces the deviations due to the truncation of the potential significantly, enabling molecular simulations with planar interfaces and a small cutoff radius.

Acknowledgment

The authors gratefully acknowledge financial support from BMBF within the SkaSim project (Grant no. 01H13005A) and from Deutsche Forschungsgemeinschaft (DFG) within the Collaborative Research Center (SFB) 926 as well as the Reinhart Koselleck Programme (Grant HA1993/15-1). They thank Jadran Vrabec and Gábor Rutkai for fruitful discussions. The present work was conducted under the auspices of the Boltzmann-Zuse Society of Computational Molecular Engineering (BZS) and the simulations were carried out on the Regional University Computing Center Kaiserslautern (RHRK) under the grant TUKL-MSWS as well as on JUQUEEN at Jülich Supercomputing Center under the grant HKL09 within the PARSIVAL scientific computing project.

References

[1] S. Eckelsbach, S. K. Miroshnichenko, G. Rutkai and J. Vrabec, in *High Performance Computing in Science and Engineering '13*, edited by W. E. Nagel, D. H. Kröner and M. M. Resch (Springer, Chur, 2013), pp. 635–646.
[2] J.-C. Neyt, A. Wender, V. Lachet and P. Malfreyt, J. Phys. Chem. B **115** (30), 9421 (2011).
[3] C. Vega and E. de Miguel, J. Chem. Phys. **126**, 154707 (2007).
[4] D. Bhatt, R. Chee, J. Newman and C. J. Radke, Curr. Opin. Colloid Interface Sci. **9** (1-2), 145 (2004).
[5] J. Alejandre, D. J. Tildesley and G. A. Chapela, J. Chem. Phys. **102** (11), 4574 (1995).
[6] S. Werth, M. Horsch and H. Hasse, Fluid Phase Equilib. **392**, 12 (2015).
[7] S. Werth, K. Stöbener, P. Klein, K.-H. Küfer, M. Horsch and H. Hasse, Chem. Eng. Sci. **121**, 110 (2015).
[8] M. P. Allen and D. J. Tildesley, *Computer Simulations of Liquids* (Clarendon Press, Oxford, 1987).
[9] B. Saager, J. Fischer and M. Neumann, Mol. Sim. **6** (1), 27 (1991).
[10] L. Onsager, J. Am. Chem. Soc. **58** (8), 1486 (1936).

[11] P. J. in't Veld, A. E. Ismail and G. S. Grest, J. Chem. Phys. **127**, 144711 (2007).
[12] R. E. Isele-Holder, W. Mitchell and A. E. Ismail, J. Chem. Phys. **137**, 174107 (2012).
[13] G. Mathias, B. Egwolf, M. Nonella and P. Tavan, J. Chem. Phys. **118** (24), 10847 (2003).
[14] D. Tameling, P. Springer, P. Bientinesi and A. E. Ismail, J. Chem. Phys. **140**, 024105 (2014).
[15] M. Mecke, J. Winkelmann and J. Fischer, J. Chem. Phys. **107** (21), 9264 (1997).
[16] J. Janeček, J. Phys. Chem. B **110** (12), 6264 (2006).
[17] S. Werth, G. Rutkai, J. Vrabec, M. Horsch and H. Hasse, Mol. Phys. **112** (17), 2227 (2014).
[18] J. W. Perram, H. G. Peterson and S. W. de Leeuw, Mol. Phys. **65** (4), 875 (1988).
[19] C. W. Glass, S. Reiser, G. Rutkai, S. Deublein, A. Köster, G. Guevara-Carrion, A. Wafai, M. Horsch, M. Bernreuther, T. Windmann, H. Hasse and J. Vrabec, Comp. Phys. Comm. **185** (12), 3302 (2014).
[20] R. W. Hockney and J. W. Eastwood, *Computer Simulations Using Particles* (Taylor & Francis, Bristol, PA, USA, 1988).
[21] A. Arnold, F. Fahrenberger, C. Holm, O. Lenz, M. Bolten, H. Dachsel, R. Halver, I. Kabadshow, F. Gähler, F. Heber, J. Iseringhausen, M. Hofmann, M. Pippig, D. Potts and G. Sutmann, Phys. Rev. E **88**, 063308 (2013).
[22] R. E. Isele-Holder, W. Mitchell, J. R. Hammond, A. Kohlmeyer and A. E. Ismail, J. Chem. Theory Comput. **9** (12), 5412 (2013).
[23] S. Deublein, P. Metzler, J. Vrabec and H. Hasse, Mol. Sim. **39** (2), 109 (2012).
[24] T. Merker, J. Vrabec and H. Hasse, Fluid Phase Equilib. **315**, 77 (2012).
[25] B. Eckl, J. Vrabec and H. Hasse, Fluid Phase Equilib. **274** (1–2), 16 (2008).
[26] B. Eckl, J. Vrabec and H. Hasse, J. Phys. Chem. B **112** (40), 12710 (2008).
[27] Y.-L. Huang, M. Heilig, H. Hasse and J. Vrabec, AIChE J. **52** (4), 1043 (2011).
[28] B. Eckl, Y.-L. Huang, J. Vrabec and H. Hasse, Fluid Phase Equilib. **260** (2), 177 (2007).
[29] J. Stoll, J. Vrabec and H. Hasse, J. Chem. Phys. **119** (21), 11396 (2003).
[30] T. Merker, J. Vrabec and H. Hasse, Soft Mater. **10** (1-3), 3 (2012).
[31] D. Cook and J. S. Rowlinson, Proc. Roy. Soc. A **219** (1138), 405 (1953).
[32] J. S. Rowlinson, Mol. Phys. **1** (4), 414 (1958).
[33] D. M. Heyes, Phys. Rev. B **49** (2), 755 (1994).
[34] M. Mecke, J. Fischer and J. Winkelmann, J. Chem. Phys. **114** (13), 5842 (2001).
[35] S. Enders, H. Kahl, M. Mecke and J. Winkelmann, J. Mol. Liq. **115** (1), 29 (2004).
[36] S. Samin, Y. Tsori and C. Holm, Phys. Rev. E **87**, 052128 (2013).
[37] W. H. Stockmayer, J. Chem. Phys. **9** (5), 398 (1941).
[38] C. G. Gray and K. E. Gubbins, *Theory of Molecular Fluids, Vol. 1: Fundamentals* (Clarendon Press, Oxford, 1984).
[39] F. Siperstein, A.L. Myers and O. Talu, Mol. Phys. **100** (13), 2025 (2002).
[40] J. H. Irving and J. G. Kirkwood, J. Chem. Phys. **18** (6), 817 (1950).
[41] C. Niethammer, S. Becker, M. Bernreuther, M. Buchholz, W. Eckhardt, A. Heinecke, S. Werth, H.-J. Bungartz, C. W. Glass, H. Hasse, J. Vrabec and M. Horsch, J. Chem. Theory Comput. **10** (10), 4455 (2014).
[42] W. Eckhardt, A. Heinecke, R. Bader, M. Brehm, N. Hammer, H. Huber, H.-G. Kleinhenz, J. Vrabec, H. Hasse, M. Horsch, M. Bernreuther, C. W. Glass, C. Niethammer, A. Bode and H.-J. Bungartz, in *Supercomputing (Proc. 28th ISC)*, no. 7905 in LNCS (Springer, Heidelberg, 2013), pp. 1–12.
[43] D. Fincham, Mol. Phys. **8** (3-5), 165 (1992).
[44] S. Werth, S. V. Lishchuk, M. Horsch and H. Hasse, Physica A **392** (10), 2359 (2013).
[45] H. Flyvberg and H. Peterson, J. Chem. Phys. **91** (1), 461 (1989).
[46] J. P. R. B. Walton, D. J. Tildesley, J. S. Rowlinson and J. R. Henderson, Mol. Phys. **48** (6), 1357 (1983).
[47] J. H. Irving and J. G. Kirkwood, J. Chem. Phys. **17** (3), 338 (1949).
[48] T. Merker, C. Engin, J. Vrabec and H. Hasse, J. Chem. Phys. **132**, 234512 (2010).
[49] J. Vrabec, J. Stoll and H. Hasse, J. Phys. Chem. B **105** (48), 12126 (2001).
[50] E. Bourasseau, M. Haboudou, A. Boutin, A. H. Fuchs and P. Ungerer, J. Chem. Phys. **118** (7), 3020 (2003).
[51] W. L. Jorgensen, D. S. Maxwell and J. Tirado-Rives, J. Am. Chem. Soc. **118** (45), 11225 (1996).
[52] M. G. Martin and J. I. Siepmann, J. Phys. Chem. B **102** (14), 2569 (1998).
[53] J. Stoll, J. Vrabec and H. Hasse, Fluid Phase Equilib. **209** (1), 29 (2003).
[54] M. E. van Leeuwen, Fluid Phase Equilib. **99**, 1 (1994).
[55] G. Gao, W. Wang and X. C. Zeng, Fluid Phase Equilib. **137**, 87 (1997).
[56] B. J. Berne and G. D. Harp, Adv. Chem. Phys. **17**, 63 (1970).
[57] M. E. van Leeuwen and B. Smit, Phys. Rev. Lett. **71** (24), 3991 (1993).

[58] J. Bartke and R. Hentschke, Phys. Rev. E **75** (6), 061503 (2007).
[59] J. J. Cerda, V. Ballenegger, O. Lenz and C. Holm, J. Chem. Phys **129**, 234104 (2008).
[60] A. P. Kudchadker, G. H. Alani and B. J. Zwolinski, Chem. Rev. **68** (6), 659 (1968).
[61] J. G. Harris, J. Phys. Chem. **96**, 5077-5086 (1992).

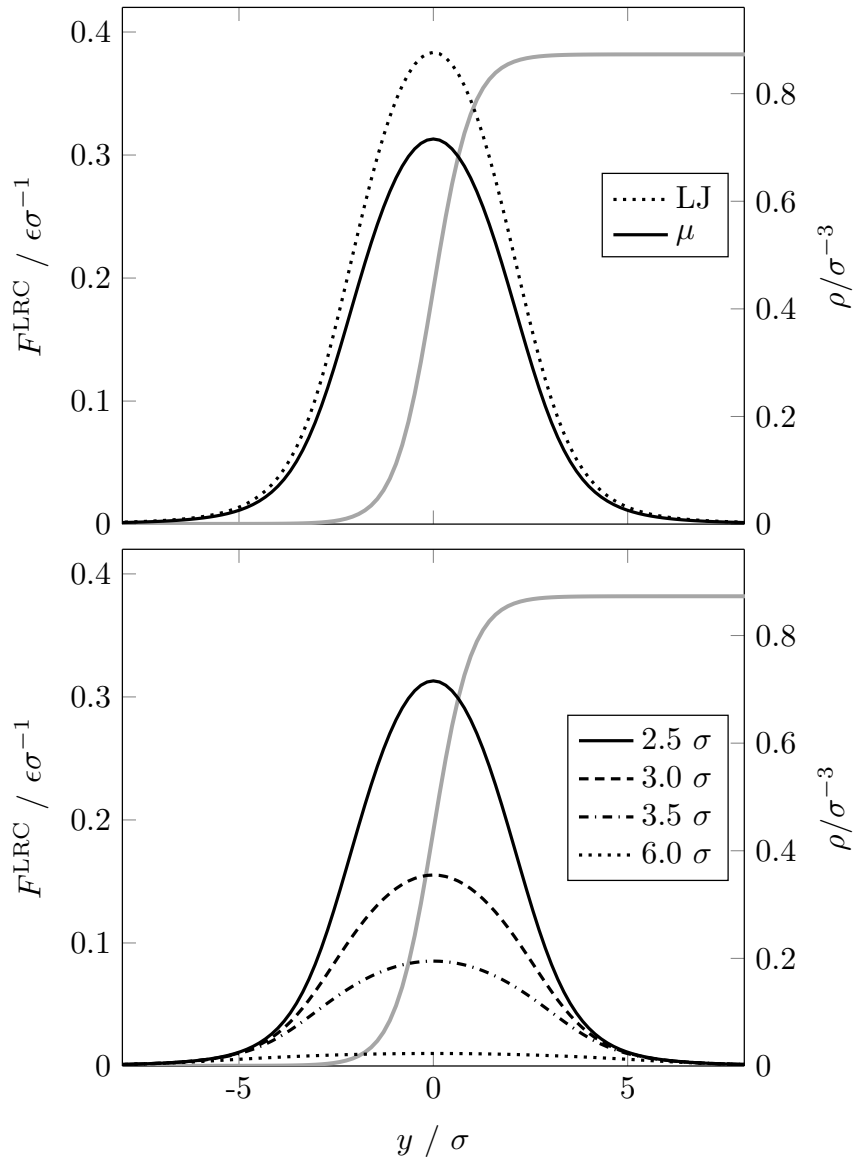

Figure 1. Density profile (gray) and long-range force correction F^{LRC} (black) of the dipole-dipole interactions over the coordinate normal to the interface for the Stockmayer fluid with $\mu^2 = 5\ \epsilon\sigma^3$ and $T = 1.28\ \epsilon/k_{\mathrm{B}}$. Comparison between the long-range force correction for the dispersive Lennard-Jones interactions and dipolar interactions for a cutoff radius of 2.5 σ (top); long-range force correction for dipolar interactions and cutoff radii of 2.5, 3.0, 3.5 and 6.0 σ (bottom). The position of the equimolar dividing surface and the maximum of F^{LRC} are at $y = 0$. The density profile is hardly influenced by the choice of the cutoff radius, cf. Figure 2, and the density profile of a molecular simulation with a cutoff radius of 6.0 σ is shown.

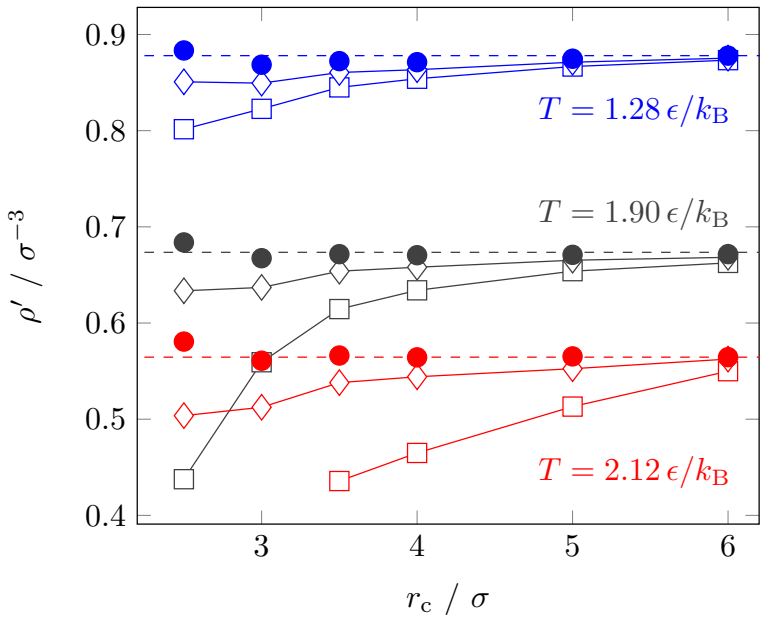

Figure 2. Saturated liquid density over the cutoff radius for the Stockmayer fluid with $\mu^2 = 5\ \epsilon\sigma^3$. Comparison between simulations without LRC (open squares), Lennard-Jones LRC (open diamonds), Lennard-Jones plus dipolar LRC (full circles) and reference values by Stoll et al. [53] (dashed lines).

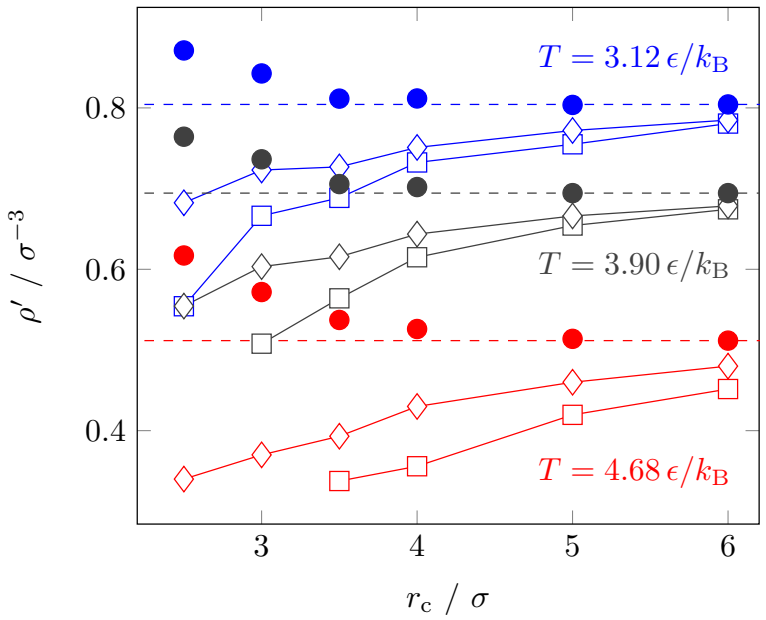

Figure 3. Saturated liquid density over the cutoff radius for the Stockmayer fluid with $\mu^2 = 16\ \epsilon\sigma^3$. Comparison between simulations without LRC (open squares), Lennard-Jones LRC (open diamonds), Lennard-Jones plus dipolar LRC (full circles) and reference values by Bartke et al. [58].

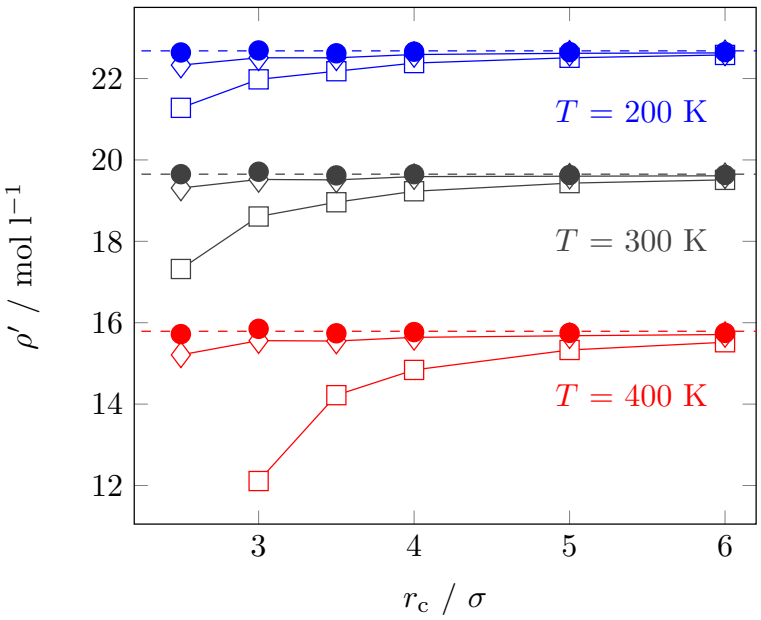

Figure 4. Saturated liquid density over the cutoff radius for ethylene oxide. Comparison between simulations without LRC (open squares), Lennard-Jones LRC (open diamonds), Lennard-Jones plus dipolar LRC (full circles) and reference values by Eckl et al. [25] (dashed lines)

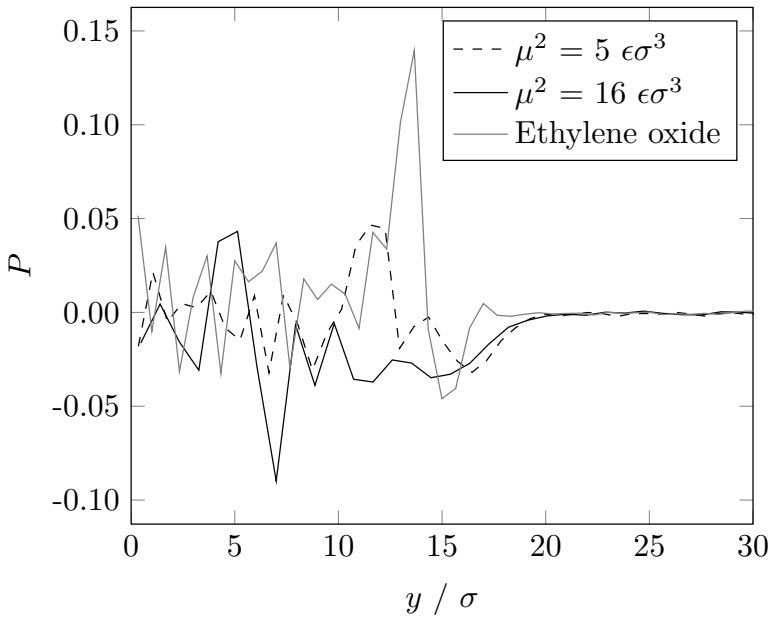

Figure 5. Orientational parameter P over coordinate normal to the interface for Stockmayer fluid with $\mu^2 = 5\ \epsilon\sigma^3$ (black dashed), $\mu^2 = 16\ \epsilon\sigma^3$ (black solid) and the ethylene oxide model by Eckl et al. [25] (gray solid).

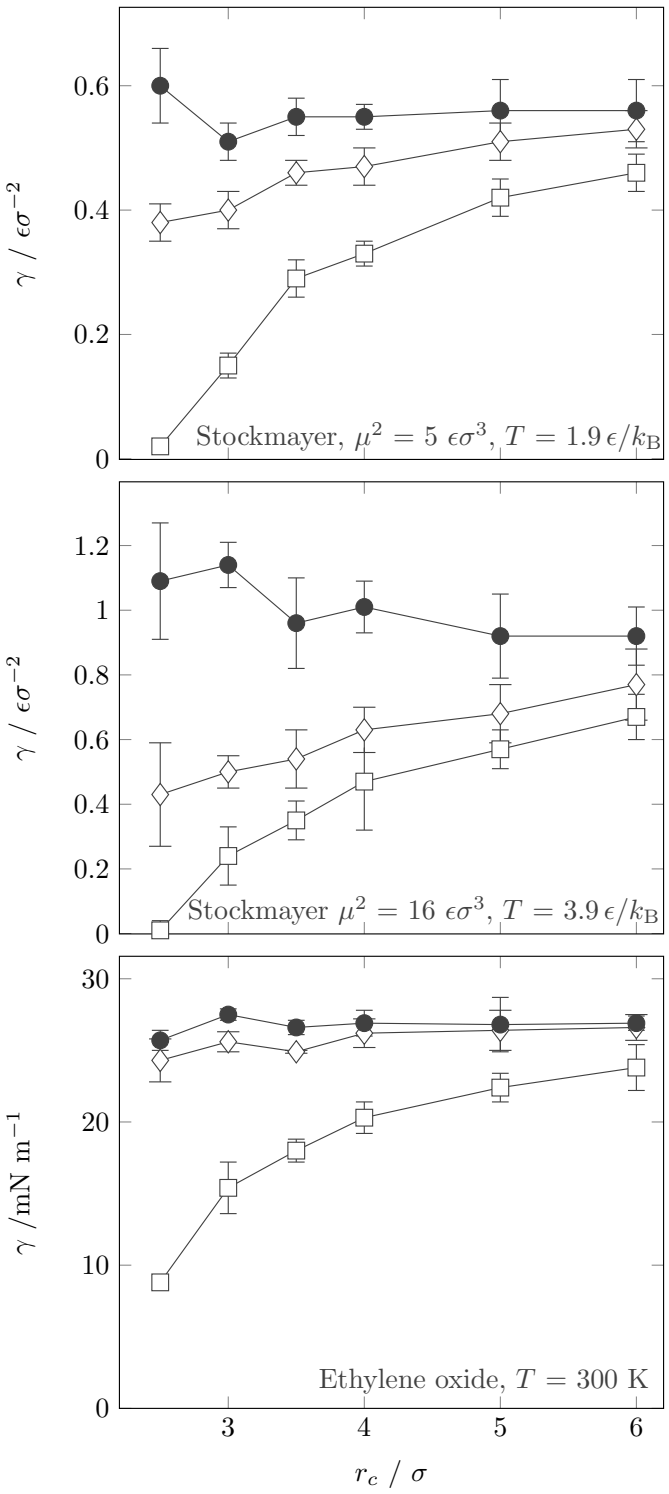

Figure 6. Surface tension over the cutoff radius for Stockmayer fluid with $\mu^2 = 5\ \epsilon\sigma^3$ (top), $\mu^2 = 16\ \epsilon\sigma^3$ (center) and the ethylene oxide model by Eckl et al. [25] (bottom). Comparison between simulations without LRC (open squares), Lennard-Jones LRC (open diamonds) and Lennard-Jones plus dipolar LRC (full circles).